Carrier-Envelope-Offset Frequency Stable 100 W-Level Femtosecond Thin-Disk Oscillator

Sebastian Gröbmeyer, Jonathan Brons, Marcus Seidel, and Oleg Pronin*

In this paper, the carrier-envelope-offset (CEO) frequency stabilization of a Kerr-lens mode-locked femtosecond oscillator with average power 105 W is presented. Intra-cavity Kerr lensing is realized in a quartz crystal that simultaneously serves as an acousto-optic loss modulator. This novel method results in a CEO frequency stable laser with high average power and a residual in-loop phase noise below 90 mrad. Furthermore, an all-solid-state bulk broadening stage is presented. The compressed, CEO frequency-stabilized output has a peak power exceeding 67 MW at a pulse duration of 40 fs and a repetition rate of 15.6 MHz. The intra-cavity peak power of the CEO frequency-stabilized oscillator is around 200 MW. These results pave the way toward compact, transportable all-solid-state drivers with high repetition rates for deep UV and XUV frequency combs and other nonlinear processes.

1. Introduction

The experimental investigation of atomic and molecular electronic structures in the deep UV and XUV ranges is limited by the currently accessible synchrotron sources,[1] and the relatively complex laser-based systems[2] and spectrometers operating in this wavelength range.[1] Among the most exciting applications in this spectral range is the spectroscopy of the 1S–2S transition of He^+ ions, a milestone that has not yet been reached. The direct detection of this atomic transition requires a coherent deep UV source emitting at around a wavelength of 60.8 nm to efficiently drive the two-photon transition.[3] Deep UV radiation is also required, for example, for a new generation of ultra-precise atomic clocks based on a transition in thorium nuclei that has only recently been shown to be in the 68–197 nm wavelength range.[4] A promising approach for accessing the desired wavelength range is the frequency upconversion of laser radiation, for example, by means of high harmonic generation (HHG) in noble gases. However, even when driven with pulses as short as 20 fs the conversion efficiency is only on the order of about 10^{-6},[5,6] although the conversion efficiency into single harmonic peaks can be increased by the use of waveguide structures in the frequency conversion process.[7] Consequently, drivers that can provide high average powers are required to compensate for the low efficiency. Until now, such systems have conventionally been based on cascaded extra-cavity amplification or enhancement cavities since the achievable power from the laser oscillator is often insufficient for direct HHG. However, these systems are often bulky and complex in design and fiber-based amplification systems in particular tend to suffer from significant high frequency (>100 kHz) intensity noise[8] that is correlated with noise in the carrier-envelope phase (CEP) as a result of the amplitude-to-phase coupling in nonlinear media. During conversion to XUV, a significant multiplication of this noise is expected,[9] which can be highly obstructive in high-precision spectroscopic applications. High-power thin-disk oscillators have been shown to exhibit excellent noise characteristics, reaching shot-noise limited performance (at >100 kHz).[10] Moreover, significant reduction in CEP flicker noise is expected for thin-disk oscillators, thanks to their relatively low repetition rate and high intra-cavity power.[11] The combination of Kerr-lens mode-locked high-power oscillators with external spectral broadening and pulse compression facilitates the generation of extremely short pulses of only a few optical cycles.[12] The stabilization of the CEP of such laser systems when operated at high average and peak powers is therefore an essential step toward the development of a highly stable, compact, transportable driver for HHG.

Thus far, several techniques for stabilizing the carrier-envelope-offset (CEO) frequency of high-power laser oscillators have been successfully demonstrated. These approaches are generally based on control of the pump power or the intra-cavity losses of the oscillator or on feed-forward schemes.[13] While control of the pump power is power scalable and therefore also applicable to thin-disk oscillators, the bandwidth of the stabilization scheme is typically limited by the cavity dynamics of the laser oscillator. For most rare-earth-doped solid-state lasers, the achievable control bandwidth is on the order of several tens of kilohertz, although it can be shifted to higher frequencies by utilizing phase

S. Gröbmeyer, Dr. J. Brons
Ludwig-Maximilians-Universität München
Am Coulombwall 1, D-85748 Garching, Germany
E-mail: sebastian.groebmeyer@physik.uni-muenchen.de
Dr. J. Brons
Trumpf Laser GmbH
Aichhalder Str. 39, D-78713 Schramberg, Germany
Dr. M. Seidel, Dr. O. Pronin
Max-Planck-Institut für Quantenoptik
Hans-Kopfermann-Str. 1, D-85748 Garching, Germany
Dr. O. Pronin
Helmut-Schmidt-Universität/Universität der Bundeswehr Hamburg
Holstenhofweg 85, D-22043 Hamburg, Germany

The ORCID identification number(s) for the author(s) of this article can be found under https://doi.org/10.1002/lpor.201800256

DOI: 10.1002/lpor.201800256

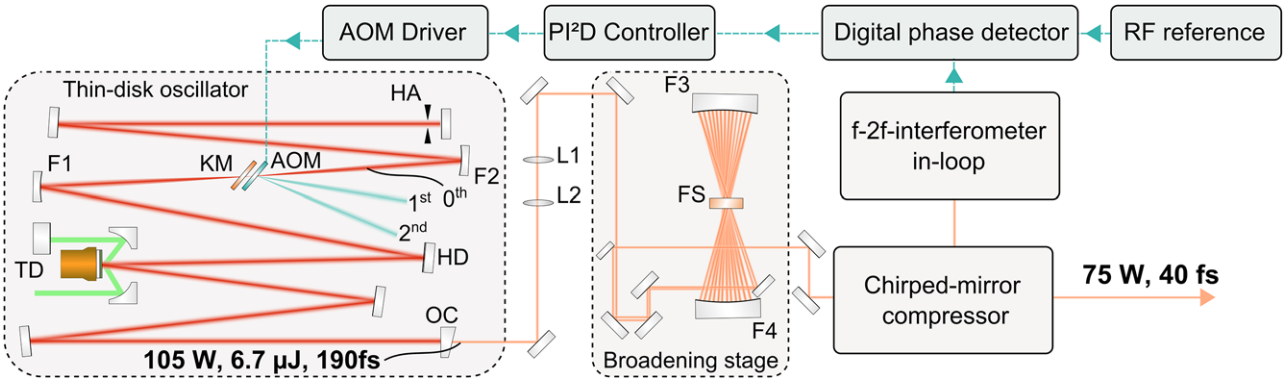

Figure 1. Schematic of the setup. The AOM is placed inside the focusing telescope as additional Kerr medium. F1–F4, focusing mirrors; FS, fused silica window; HA, hard aperture; HD, highly dispersive mirror; KM, Kerr medium; L1, L2, mode-matching lenses; OC, 15% output coupler; TD, thin disk.

lead filters in the phase-locked loop (PLL).[14,15] CEO frequency stabilization by pump power control has been demonstrated experimentally, for example, in previous work[14] by implementing a dual-wavelength pumping scheme, although only with a residual in-loop phase noise of 390 mrad due to the limited control bandwidth.

This limitation can be overcome by utilizing intra-cavity loss modulation instead of pump power control, as has successfully been demonstrated in fiber oscillators[16] utilizing electro-optic modulators, in thin-disk oscillators[12] using acousto-optic modulators (AOMs) and in bulk lasers using cw-pumped semiconductor saturable-absorber mirrors (SESAMs) as opto-optical modulators.[17,18] Until now, the CEO frequency stabilization of Kerr-lens mode-locked thin-disk (TD) oscillators using intra-cavity loss modulation has only been realized in oscillators with average output powers of below 50 W and, more importantly, with intra-cavity peak powers of below 30 MW using an AOM for CEO control. In the experiments presented in previous work,[12] a residual in-loop phase noise of 180 mrad was reported using the intra-cavity loss modulation approach. However, scaling the concept to higher power would necessitate an increased spot size inside the AOM and therefore reduce the control bandwidth, thus, likely compromising the achievable in-loop phase noise. Furthermore, the additional self-focusing inside the AOM crystal used for loss modulation can counteract the main Kerr-lens mode-locking (KLM) mechanism and degrade the mode-locking performance. This becomes particularly significant when the concept is applied to high-power oscillators, since in this case the intra-cavity peak power rises substantially and the nonlinear contribution of the AOM material becomes important even for large beam diameters inside the AOM.

Feed-forward stabilization has been demonstrated to work well for low-power seed lasers based on Ti:sapphire bulk materials.[13] However, several limitations must be faced when applying the concept to high-power lasers. The concept relies on utilizing the first diffraction order beam from an AOM which requires high diffraction efficiency. However, for a high-power beam incident on the AOM, the beam diameter needs to be large to avoid self-focusing and thermal lensing. This aspect severely limits both the achievable diffraction efficiencies as well as the accessible modulation bandwidth. Furthermore, the initial passive stability of the CEO frequency needs to be very high to prevent significant beam-pointing fluctuations at the first diffraction order of the AOM.[19] This makes the overall system complex in terms of design, requires the implementation of additional feedback loops[20] and limits the applicability of this approach for high-power lasers.

We demonstrate a novel approach for CEO frequency stabilization by realizing KLM in a quartz crystal that simultaneously serves as an intra-cavity acousto-optic loss modulator. By placing the AOM in the beam focus inside the oscillator, a large control bandwidth of 230 kHz was achieved. Furthermore, the self-focusing introduced by the Kerr effect inside the AOM is used to initiate and stabilize the Kerr-lens mode-locked operation. Using the technique presented here, a residual in-loop phase noise of 90 mrad (1 Hz–500 kHz) was reached at an unprecedented high average output power of 105 W and an intra-cavity peak power of more than 200 MW, thus representing the highest average power of a CEO frequency stable laser available today. This corresponds to a CEO frequency-stabilized intra-cavity peak power that is improved by more than a factor of seven and a simultaneous reduction of the in-loop phase noise by a factor of two when compared to the state of the art.[12] Furthermore, all-solid-state spectral broadening of the oscillator output is realized in a multi-pass cell (MPC) resulting in a peak power of 67 MW with a pulse duration of 40 fs after recompression. These parameters are closely comparable to state-of-the-art CEP-stable, Ti:sapphire seeded fiber amplifier systems,[21,22] although, with significantly reduced complexity and size.

2. Results

2.1. Acousto-Optic Loss Modulation Inside the Kerr Medium

The experimental setup is sketched in **Figure 1**. The Kerr-lens mode-locked Yb:YAG TD oscillator used here is a slightly modified version of the oscillator described in previous work.[23] The TD oscillator was set to emit an average output power of 105 W, delivering 190 fs pulses with pulse energy 6.7 μJ at a repetition rate of 15.6 MHz and central wavelength 1030 nm. An AOM was incorporated as a Kerr medium (see the Experimental Section) to control the CEO frequency via intra-cavity loss modulation.[12] The AOM operates in the Raman–Nath diffraction regime (see

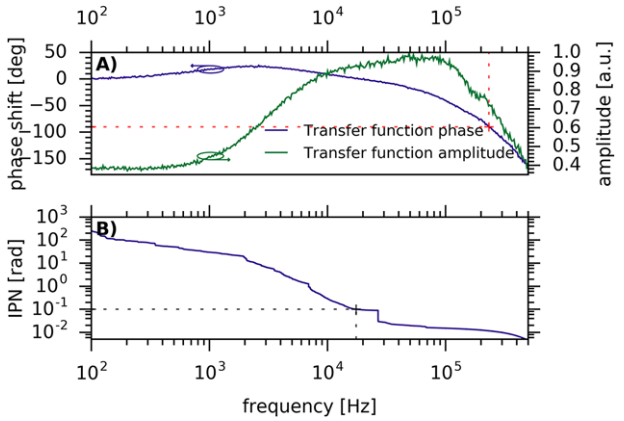

Figure 2. Transfer function of the oscillator output power. A) Phase and amplitude transfer functions of the oscillator output power in response to the AOM modulation measured with Zurich Instruments UHF lock-in amplifier. The dashed red line indicates the frequency at which a phase shift of 90° is accumulated. B) Integrated phase noise (IPN) of the free-running CEO beat. The dashed blue line indicates the frequency at which an IPN of 100 mrad is reached.

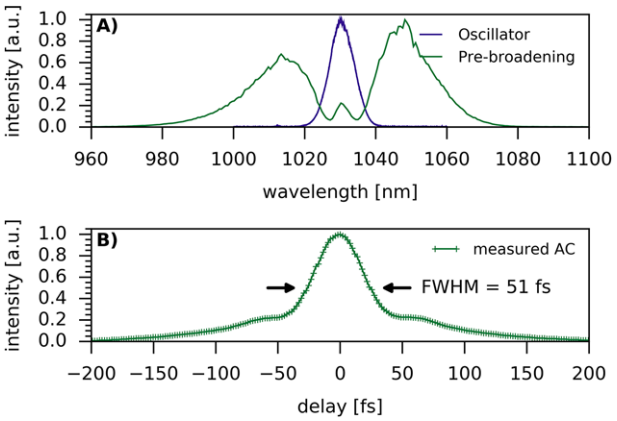

Figure 3. Broadening stage output. A) Measured spectra at the output of the oscillator (blue) and at the output of the Herriott-type MPC (green) measured with a grating spectrometer (Ocean Optics). B) Autocorrelation measured at the output of the chirped-mirror compressor after the MPC.

the schematic diffraction in Figure 1) with a diffraction efficiency into the higher orders that is estimated at well below 1%.

To characterize the performance of the AOM when implemented as a Kerr medium, the transfer function of the oscillator output power when modulating the intra-cavity power using the AOM was measured with a lock-in amplifier (Zurich Instruments UHF, **Figure 2**A). A phase lag of 90° was reached at ≈230 kHz allowing for CEO frequency control over a wide frequency band. The phase transfer function shows a small phase shift of ≈25° centered at around 2 kHz which presumably originates from the resonance close to the relaxation oscillation frequency of the oscillator. The amplitude transfer function shows a distinctive high-pass filtering behavior that can be explained by taking a closer look at the upper-state lifetime of the gain medium; for Yb:YAG, the upper-state lifetime is ≈1 ms. Therefore, at frequencies below 1 kHz, the slow modulation of intra-cavity power introduced by the AOM can be counteracted by the dynamic gain saturation of the laser medium which effectively reduces the modulation amplitude.[16] In contrast, the modulation amplitude for frequencies exceeding 1 kHz is only slightly reduced since the power oscillations are too fast to be followed by the upper-state population of the gain medium. It should be noted that the amplitude modulation at frequencies below 1 kHz is damped by only about −7 dB which can easily be compensated by the frequency dependent feedback in the servo-loop.

To assess whether the available control bandwidth is sufficient for the stabilization of the CEO frequency, the noise characteristics of the free-running CEO beat obtained from an f-to-2f interferometer were analyzed using the method presented in previous work[14] (see Supporting Information for details). Evaluation of the integrated phase noise (IPN) of the free-running CEO beat (Figure 2B) showed that a modulation bandwidth of more than 20 kHz is required to obtain a residual phase noise level below 100 mrad. This is readily provided by the AOM, exceeding the minimum desired bandwidth by an order of magnitude.

2.2. All-Solid-State Bulk Broadening Stage

Since the efficiency of driving most nonlinear processes benefits from high peak power and short pulse duration, about 80 W of the oscillator output was sent to a spectral broadening stage, which consisted of two lenses for mode matching and a subsequent Herriott-type MPC. This Herriott cell is comprised of two concave mirrors and a bulk window (see FS, Figure 1) placed centrally between them. The MPC forms a quasi-waveguide for a beam whose mode is matched to the cell eigenmode and allows for a large number of beam passes through the window before being coupled out. As has been demonstrated in various works,[24,25] this scheme can be used to efficiently broaden the laser spectrum while maintaining a high beam quality and high throughput. The MPC utilized here comprised 31 passes through an AR-coated fused silica plate with a thickness of 6.35 mm. The broadened spectrum (**Figure 3**A) was subsequently sent to a chirped-mirror compressor, effectively reducing the pulse duration to 40 fs (deduced from autocorrelation measurement, as shown in Figure 3B assuming a Gaussian temporal profile for the main pulse feature). The peak power could thus be increased to 67 MW, taking into account the power loss into the pedestal, which is caused by residual uncompensated second- and higher-order dispersion. Due to imperfect mode matching, the input power of the MPC was limited to 80 W, since higher input powers resulted in white light generation inside the fused silica plate. It should be noted that supercontinuum generation in highly nonlinear fibers leads to a loss of temporal coherence if pulses exceeding durations of about 100 fs are used.[26] The pulse compression therefore also ensured that temporal coherence was maintained throughout the subsequent supercontinuum generation process.

2.3. CEO Frequency Stabilization

For the phase-stabilization experiments, about 130 mW of the broadening stage output was sent to a home-built f-to-2f

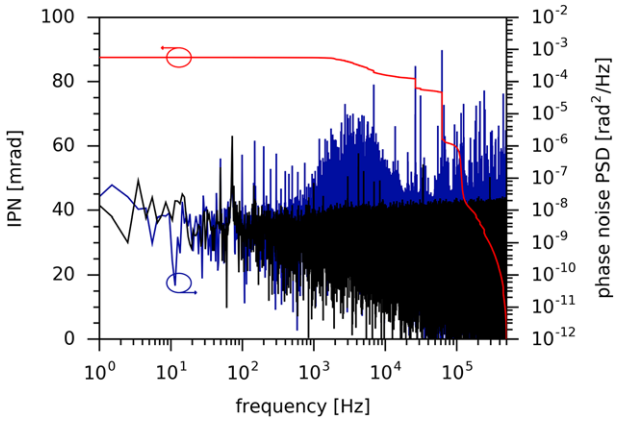

Figure 4. Residual in-loop phase noise. The blue curve shows the phase noise power spectral density (PSD) of the CEO beat assessed from the recorded error signal. The IPN from 500 kHz to 1 Hz is displayed in red. The noise floor PSD of the oscilloscope (without digital phase detector) is shown in black.

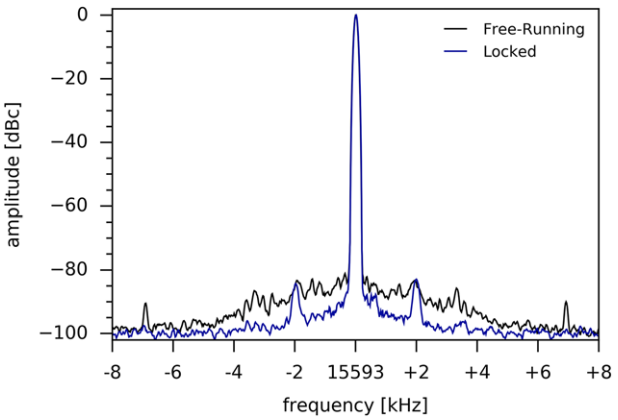

Figure 5. Oscillator phase noise reduction. Comparison of the phase noise of the repetition rate of the oscillator for the free-running case (black) and for the case of locked CEO frequency (blue, both measured with Agilent E4447A RF Analyzer, 100 Hz RBW). Due to a strong amplitude-to-phase coupling in the Kerr medium (AOM) inside the oscillator, locking of the CEO frequency likewise results in a clear reduction of the laser phase noise.

interferometer (see Experimental Section), and the CEO frequency was subsequently locked to an external RF reference. A minimum residual in-loop phase noise of 90 mrad (1 Hz–500 kHz) was observed. The power spectral density (PSD) of the detected error signal and the IPN are shown in **Figure 4**. The spike at 26.4 kHz is also visible in the phase noise of the free-running beat note; this presumably stems from the oscillator although its exact origin is yet unknown. A second spike at 62.5 kHz and excess noise in the range 100–500 kHz was found to be inscribed by the digital phase detector (DPD) used for the experiments. This noise could potentially be reduced by using a different phase detector with an intrinsically lower noise floor.

2.4. Reduction of the Repetition Rate Phase Noise

Due to strong amplitude-to-phase coupling in the Kerr medium the reduced phase noise during CEO frequency-stabilized operation was also expected to manifest itself in a reduction of the oscillator phase and intensity noise. This was verified by analyzing the phase noise of the pulse repetition frequency, which was measured with a high dynamic-range RF Analyzer (**Figure 5**). From Figure 5, it can be seen that the phase noise around the carrier decreases once the CEO frequency is locked, revealing previously hidden sidebands around ± 2 kHz. These sidebands can be attributed to the interplay between the AOM modulation and the gain dynamics of the oscillator which is masked by the generally higher low-frequency noise in the unlocked case. The results indicate a significant coupling of the CEO phase noise to the oscillator repetition rate phase noise which might facilitate the use of an AOM both as a Kerr medium and in the stabilization of repetition rate phase noise. However, this cross-talk behavior between the CEO frequency noise and repetition rate phase noise requires more careful analysis, especially in the low-frequency range. The oscillator intensity noise and its coupling to the phase noise should also be characterized in future work.

3. Discussion

Although no out-of-loop noise measurements were performed, the residual out-of-loop phase noise is expected to be somewhat higher than the in-loop noise. According to previously reported results,[12] the difference in the phase noise can be a factor of two to three. The main differences in phase noise performance between the in-loop and out-of-loop cases originated from beam-pointing fluctuations, which are converted to phase noise by amplitude-to-phase coupling inside the highly nonlinear photonic crystal fiber (PCF), and a general noise amplification during the supercontinuum generation.[27] The conceptual similarity of the two experiments therefore suggests a comparable difference between in-loop and out-of-loop noise in the existing setup.

To ultimately drive CEP-sensitive effects such as electron emission from nanotips[28] or optical-field-induced currents in dielectrics,[29] CEO frequency stabilization to an arbitrary RF reference is not sufficient, and an offset-free stabilization method should be applied. Recently, Okubo et al.[30] have demonstrated an offset-free self-referencing scheme that allows the generation of zero offset frequency combs using a conventional f-to-2f interferometer in conjunction with an additional photodiode for subtraction of the repetition rate signal from the RF-spectrum. This method could easily be adapted for the presented stabilization scheme, and would allow the generation of truly CEP-stable pulses without impairing the noise characteristics of the phase-locking method presented here.

In the existing setup, the duration of CEO frequency stable operation was limited to several minutes due to beam-pointing drifts in the laser system, which could be attributed to the warming up of the AOM due to the applied RF power. This can be mitigated by applying the RF power to the AOM over an extended period of time (about half an hour) to allow the AOM to thermally stabilize before locking the CEO frequency. Residual beam-pointing instabilities are currently being addressed by progressing to a fiber-free method of generating the beat signal which

is expected to exhibit a significantly reduced sensitivity to beam-pointing fluctuations and improved overall thermal stability of the external pulse compression scheme and the interferometer (see Supporting Information).

It is instructive to discuss the average and peak power scalability of the approach implemented here. A Kerr-lens mode locked oscillator operating with 1 kW intra-cavity average power was demonstrated in previous work[23] with a sapphire plate as a Kerr medium. In our experience, crystalline quartz shows similar thermo-optical performance to that of sapphire, and thus should be scalable toward an intra-cavity average power of several kilowatts. This view is also supported by the currently implemented pump diodes providing an average output power of 3 kW and driven by a 6.3 kW power supply. The peak power inside Kerr-lens mode locked TD oscillators scales linearly with the beam size in the Kerr medium, as was empirically demonstrated in previous work.[31] The beam diameter of 300 μm corresponds to a maximum peak power of about 400 MW. The beam diameter is here defined at the center of the stability zone and is somewhat smaller in practice. Thus, scaling the intra-cavity peak power by an order of magnitude (4 GW) would result in a beam diameter below 3 mm and an AOM control bandwidth of approximately an order of magnitude lower than in the case presented here, that is ≈20–30 kHz. This control bandwidth is sufficient to bring the oscillator CEO frequency noise down to <0.5 rad. It is interesting to note that, applying the same scaling rules to KLM bulk oscillators with relatively low intra-cavity peak power levels, and thus very small beam diameters in a Kerr medium (≈30 μm), should result in a control bandwidth exceeding 1 MHz.

One of the main applications for Kerr-lens mode-locked TD oscillators is the development of coherent XUV sources via HHG, for example, in gas jets.[32] XUV generation at megahertz repetition rates, which allows nonlinear compression in Kagome PCFs to reach the required low pulse durations of around 30 fs, was demonstrated by Hädrich et al.,[33] showing an improvement in the XUV photon flux in a single harmonic of almost four orders of magnitude compared to previous experiments.[34] The presented laser system can provide closely comparable output parameters (40 fs, 67 MW) when compared to this work,[33] although with vastly reduced complexity and size and in combination with CEO frequency stabilization. This experimental demonstration will therefore pave the way for a new class of oscillator-based XUV drivers that can be utilized for frequency comb and phase-sensitive high-field experiments. Importantly, intra-cavity nonlinear processes such as HHG can also be used in an analogous way to those used in previous demonstrations by other groups,[35,36] thanks to the high peak power level inside of the oscillator and readily available methods of pulse shortening beyond the emission bandwidth limit to below 50 fs in KLM[37] and distributed KLM regimes.[38]

4. Conclusion

In summary, we have presented a high average power CEO frequency stable laser and high peak power CEO-frequency stable oscillator. By exploiting the nonlinear properties of the AOM material we were able to implement Kerr lensing inside the AOM crystal while at the same time utilizing its acousto-optical properties to introduce intra-cavity loss modulation. In this way, a large control bandwidth of 230 kHz could be achieved which is comparable to the bandwidths reached using a feed-forward scheme.[13] The TD oscillator was CEO frequency stabilized with a residual in-loop phase noise below 90 mrad at an average output power of 105 W. In combination with the power scaling laws for TD oscillators, we believe that this novel, power-scalable approach to CEO frequency stabilization will allow the development of mode-locked high-power TD oscillators providing a peak power of more than 100 MW and an average power in the kW regime. Additionally, by using a Herriot-cell type broadening scheme, pulses were generated with a peak power of 67 MW and an average power of 75 W at a pulse duration as short as 40 fs with a repetition rate of 15.6 MHz. Further steps are being taken toward the realization of all-bulk-broadening toward sub-15 fs pulse duration[39] in combination with 2f-to-3f interferometers for characterizing in-loop noise and minimizing the out-of-loop noise as well as improving the long-term stability.

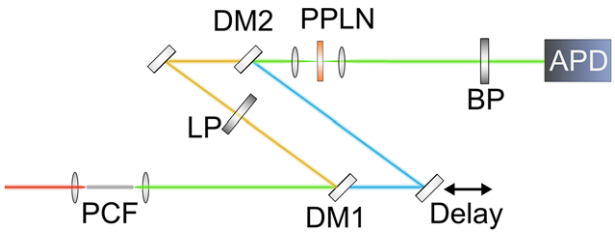

Figure 6. F-to-2f interferometer layout. APD, avalanche photodetector; BP, bandpass filter; DM, dichroic mirror; LP, longpass filter; PCF, photonic crystal fiber; PPLN, periodically poled lithium niobate for second harmonic generation.

5. Experimental Section

TD Oscillator: The AOM used as a Kerr medium had a thickness of ≈3 mm and was placed at Brewster's angle inside the focusing telescope of the oscillator, replacing the originally implemented 5 mm sapphire plate as the Kerr medium.[23] A 3 mm thick quartz plate was placed close to the AOM as an additional Kerr medium to assimilate the overall Kerr-lensing effect of the original configuration. The exact separation distance between the AOM and the quartz-plate was found to be uncritical due to the long Rayleigh length of the focused beam of radius ≈300 μm. Due to the decoupling of the Kerr and gain media in mode-locked thin-disk oscillators, this modification was made without requiring further changes to the oscillator. The reduction in output power compared to previous work[23] was realized by changing the position of the Kerr medium and was carried out in order to optimize the passive stability of the output CEO frequency, for example, to reduce the slow fluctuations in the CEO frequency. Otherwise, nearly the same peak- and average-power levels (60 MW, 150 W) could be reached with the presented AOM/Kerr medium combination.

F-to-2f Interferometer: The layout of the f-to-2f interferometer utilized here is depicted in **Figure 6**. To generate an octave-spanning spectrum, ≈130 mW of the compressed pre-broadening stage output was sent into a highly nonlinear PCF (NKT Photonics SC-3.7-975) to generate a supercontinuum. A home-built f-to-2f interferometer was used for the detection of the CEO frequency, where a Mach–Zehnder interferometer layout was chosen over a quasi-common path geometry. Although a common path can significantly reduce the contributions from air fluctuation and mechanical vibrations to the measured phase noise, the layout chosen here facilitates additional filtering inside the interferometer arms, which was necessary to

avoid saturation of the avalanche photodetector (APD). The red part of the spectrum was separated with a dichroic mirror and was longpass filtered at 1200 nm before being recombined with the blue part. The blue part had a variable delay to ensure the temporal overlap of the fundamental and second harmonic components on the APD. For the generation of the second harmonic components, a periodically poled lithium niobate crystal was used. Both fundamental and second harmonic beams were filtered with a bandpass filter centered at 690 nm with a full width at half maximum (FWHM) of 10 nm before impinging on the detector, thus reducing detector saturation due to non-overlapping spectral components.

Phase-Locked Loop: In order to lock the CEO frequency, the free-running beat signal was shifted to 10.7 MHz by slightly adjusting the pump power. The CEO frequency was bandpass filtered and amplified by +60 dB before being compared to an externally applied RF signal (10.7 MHz, from a Marconi 2022D Signal Generator) in a $\pm 16\pi$ DPD (home built). The resulting error signal was split, with half the power being sent to a proportional–integral–derivative (PID) controller (Vescent-Photonics D2-125) and the other half being used for monitoring the locking performance on a digital oscilloscope. The servo signal generated in the PID controller was then applied to the modulation input of the AOM driver. By varying the corner frequencies of the integral parts (first integrator set to 50 kHz, second integrator 5 kHz), the corner frequency of the derivative part (set to 20 kHz), and the proportional gain of the PID controller, a tight lock of the CEO frequency could be achieved.

Supporting Information

Supporting Information is available from the Wiley Online Library or from the author.

Acknowledgements

The authors acknowledge support from Dominik Bauer and Dirk Sutter from TRUMPF Laser GmbH for the thin-disk technology. The authors also gratefully acknowledge support from and fruitful discussions with Ferenc Krausz. This work was funded by the Munich-Centre for Advanced Photonics (MAP) and the Centre for Advanced Laser Applications (CALA).

Conflict of Interest

The authors declare no conflict of interest.

Keywords

laser stabilization, mode-locked lasers, pulse compression, ultrafast lasers

Received: October 3, 2018
Revised: December 12, 2018
Published online: January 11, 2019

[1] N. de Oliveira, M. Roudjane, D. Joyeux, D. Phalippou, J.-C. Rodier, L. Nahon, *Nat. Photonics* **2011**, *5*, 149.
[2] P. Rupper, F. Merkt, *Rev. Sci. Instrum.* **2004**, *75*, 613.
[3] M. Herrmann, M. Haas, U. D. Jentschura, F. Kottmann, D. Leibfried, G. Saathoff, C. Gohle, A. Ozawa, V. Batteiger, S. Knünz, N. Kolachevsky, H. A. Schüssler, T. W. Hänsch, T. Udem, *Phys. Rev. A* **2009**, *79*, 052505.
[4] L. von der Wense, B. Seiferle, M. Laatiaoui, J. B. Neumayr, H. J. Maier, H. F. Wirth, C. Mokry, J. Runke, K. Eberhardt, C. E. Dullmann, N. G. Trautmann, P. G. Thirolf, *Nature* **2016**, *533*, 47.
[5] S. Hädrich, R. Jan, M. Krebs, S. Demmler, A. Klenke, A. Tünnermann, J. Limpert, *J. Phys. B: At., Mol. Opt. Phys.* **2016**, *49*, 172002.
[6] C. M. Heyl, C. L. Arnold, A. Couairon, A. L'Huillier, *J. Phys. B: At., Mol. Opt. Phys.* **2017**, *50*, 013001.
[7] A. Rundquist, C. G. Durfee Iii, Z. Chang, C. Heme, S. Backus, M. M. Murnane, H. C. Kapteyn, *Opt. Photonics News* **1998**, *9*, 54.
[8] M. Wunram, P. Storz, D. Brida, A. Leitenstorfer, *Opt. Lett.* **2015**, *40*, 823.
[9] C. Benko, T. K. Allison, A. Cingöz, L. Hua, F. Labaye, D. C. Yost, J. Ye, *Nat. Photonics* **2014**, *8*, 530.
[10] M. Huber, W. Schweinberger, F. Stutzki, J. Limpert, I. Pupeza, O. Pronin, *Opt. Express* **2017**, *25*, 22499.
[11] Y. Song, F. Lücking, B. Borchers, G. Steinmeyer, *Opt. Lett.* **2014**, *39*, 6989.
[12] O. Pronin, M. Seidel, F. Lucking, J. Brons, E. Fedulova, M. Trubetskov, V. Pervak, A. Apolonski, T. Udem, F. Krausz, *Nat. Commun.* **2015**, *6*, 6988.
[13] S. Koke, C. Grebing, H. Frei, A. Anderson, A. Assion, G. Steinmeyer, *Nat. Photonics* **2010**, *4*, 462.
[14] M. Seidel, J. Brons, F. Lucking, V. Pervak, A. Apolonski, T. Udem, O. Pronin, *Opt. Lett.* **2016**, *41*, 1853.
[15] T. Balčiūnas, O. D. Mücke, P. Mišeikis, G. Andriukaitis, A. Pugžlys, L. Giniūnas, R. Danielius, R. Holzwarth, A. Baltuška, *Opt. Lett.* **2011**, *36*, 3242.
[16] C. C. Lee, C. Mohr, J. Bethge, S. Suzuki, M. E. Fermann, I. Hartl, T. R. Schibli, *Opt. Lett.* **2012**, *37*, 3084.
[17] M. Hoffmann, S. Schilt, T. Südmeyer, *Opt. Express* **2013**, *21*, 30054.
[18] S. Hakobyan, V. J. Wittwer, K. Gürel, A. S. Mayer, S. Schilt, T. Südmeyer, *Opt. Lett.* **2017**, *42*, 4651.
[19] B. Borchers, A. Anderson, G. Steinmeyer, *Laser Photonics Rev.* **2014**, *8*, 303.
[20] B. Borchers, S. Koke, A. Husakou, J. Herrmann, G. Steinmeyer, *Opt. Lett.* **2011**, *36*, 4146.
[21] T. Saule, S. Holzberger, O. De Vries, M. Plötner, J. Limpert, A. Tünnermann, I. Pupeza, *Appl. Phys. B* **2017**, *123*, 17.
[22] J. Rothhardt, S. Hädrich, J. C. Delagnes, E. Cormier, J. Limpert, *Laser Photonics Rev.* **2017**, *11*, 1700043.
[23] J. Brons, V. Pervak, D. Bauer, D. Sutter, O. Pronin, F. Krausz, *Opt. Lett.* **2016**, *41*, 3567.
[24] J. Schulte, T. Sartorius, J. Weitenberg, A. Vernaleken, P. Russbueldt, *Opt. Lett.* **2016**, *41*, 4511.
[25] J. Weitenberg, T. Saule, J. Schulte, P. Rußbüldt, *IEEE J. Quantum Electron.* **2017**, *53*, 1.
[26] J. M. Dudley, G. Genty, S. Coen, *Rev. Mod. Phys.* **2006**, *78*, 1135.
[27] N. R. Newbury, B. R. Washburn, K. L. Corwin, R. S. Windeler, *Opt. Lett.* **2003**, *28*, 944.
[28] M. Krüger, M. Schenk, P. Hommelhoff, *Nature* **2011**, *475*, 78.
[29] T. Paasch-Colberg, A. Schiffrin, N. Karpowicz, S. Kruchinin, Ö. Sağlam, S. Keiber, O. Razskazovskaya, S. Mühlbrandt, A. Alnaser, M. Kübel, V. Apalkov, D. Gerster, J. Reichert, T. Wittmann, J. V. Barth, M. I. Stockman, R. Ernstorfer, V. S. Yakovlev, R. Kienberger, F. Krausz, *Nat. Photonics* **2014**, *8*, 214.
[30] S. Okubo, A. Onae, K. Nakamura, T. Udem, H. Inaba, *Optica* **2018**, *5*, 188.
[31] J. Brons, V. Pervak, E. Fedulova, D. Bauer, D. Sutter, V. Kalashnikov, A. Apolonskiy, O. Pronin, F. Krausz, *Opt. Lett.* **2014**, *39*, 6442.
[32] T. Südmeyer, S. V. Marchese, S. Hashimoto, C. R. E. Baer, G. Gingras, B. Witzel, U. Keller, *Nat. Photonics* **2008**, *2*, 599.
[33] S. Hädrich, M. Krebs, A. Hoffmann, A. Klenke, J. Rothhardt, J. Limpert, A. Tünnermann, *Light: Sci. Appl.* **2015**, *4*, e320.
[34] A. Vernaleken, J. Weitenberg, T. Sartorius, P. Russbueldt, W. Schneider, S. L. Stebbings, M. F. Kling, P. Hommelhoff, H.-D. Hoffmann, R. Poprawe, F. Krausz, T. W. Hänsch, T. Udem, *Opt. Lett.* **2011**, *36*, 3428.

[35] F. Labaye, M. Gaponenko, V. J. Wittwer, A. Diebold, C. Paradis, N. Modsching, L. Merceron, F. Emaury, I. J. Graumann, C. R. Phillips, C. J. Saraceno, C. Kränkel, U. Keller, T. Südmeyer, *Opt. Lett.* **2017**, *42*, 5170.
[36] E. Seres, J. Seres, C. Spielmann, *Opt. Express* **2012**, *20*, 6185.
[37] C. Paradis, N. Modsching, V. J. Wittwer, B. Deppe, C. Kränkel, T. Südmeyer, *Opt. Express* **2017**, *25*, 14918.
[38] J. Zhang, J. Brons, M. Seidel, D. Bauer, D. Sutter, V. Pervak, V. Kalashnikov, Z. Wei, A. Apolonski, F. Krausz, O. Pronin, in *Advanced Solid State Lasers*, OSA Technical Digest (online), Optical Society of America **2015**, ATh4A.7.
[39] K. Fritsch, M. Poetzlberger, V. Pervak, J. Brons, O. Pronin, *Opt. Lett.* **2018**, *43*, 4643.